Journal of Solid State Chemistry 183 (2010) 2174–2182

Contents lists available at ScienceDirect

Journal of Solid State Chemistry

journal homepage: www.elsevier.com/locate/jssc

# Syntheses, structures and properties of silver(I) complexes with flexible 1,3,5-tris(pyridylmethoxyl)benzene ligands

Gang Wu [a,b], Xiao-Feng Wang [a], Taka-aki Okamura [c], Min Chen [a], Wei-Yin Sun [a,*], Norikazu Ueyama [c]

[a] Coordination Chemistry Institute, State Key Laboratory of Coordination Chemistry, School of Chemistry and Chemical Engineering, Nanjing National Laboratory of Microstructures, Nanjing University, Nanjing 210093, China
[b] Department of Chemistry and Life Science, Chuzhou University, Chuzhou 239012, China
[c] Department of Macromolecular Science, Graduate School of Science, Osaka University, Toyonaka, Osaka 560-0043, Japan

ARTICLE INFO

*Article history:*
Received 7 April 2010
Received in revised form
10 July 2010
Accepted 19 July 2010
Available online 24 July 2010

*Keywords:*
Anion-exchange properties
Crystal structure
Photoluminescence
Silver(I) complex

ABSTRACT

Five new silver(I) complexes $[Ag_2(L_2)_2](BF_4)_2 \cdot CH_3CN \cdot CH_3OH$ (**1**), $[Ag(L_2)(CF_3SO_3)]$ (**2**), $[Ag(L_3)]ClO_4 \cdot CH_3OH$ (**3**), $[Ag_2(L_3)_2](CF_3SO_3)_2 \cdot CH_3CN \cdot CH_3OH \cdot H_2O$ (**4**) and $[Ag(L_3)]PF_6 \cdot 2CH_3CN$ (**5**) [$L_2$=1,3,5-tris(2-pyridylmethoxyl)benzene, $L_3$=1,3,5-tris(3-pyridylmethoxyl)benzene] were synthesized and characterized by single crystal X-ray diffraction analyses. In complexes **1**–**5**, ligands $L_2$ and $L_3$ show different conformations and act as three-connectors, while the Ag(I) atom serves as three-connecting node to result in the formation of 2D and 3D frameworks. Complexes **1** and **2** with different counteranions have similar 2D network structure with the same $(4,8^2)$ topology. Complex **3** has a 3D structure with (10,3)-a topology while complexes **4** and **5** have the same 2D (6,3) topological structure. The results showed that the structure of organic ligands and counteranions play subtle but important role in determining the structure of the complexes. In addition, the photoluminescence and anion-exchange properties of the complexes were investigated in the solid state at room temperature.



## 1. Introduction

The assembly of building blocks into chains, networks and other supramolecular architectures with specific structures and topologies via coordination interactions is a major area of current research [1,2]. Architectures with specific structural motifs can be achieved by careful selection of organic ligands with suitable coordinating groups, metal centers with definite coordination geometry and reaction conditions [1b,3]. Such approach is using coordination interactions to generate primary framework which can be further organized into supramolecular architectures through weak non-covalent interactions, such as hydrogen bonding, C–H$\cdots\pi$ and $\pi$–$\pi$ interactions [4]. This strategy has been proved to be an efficient and reliable method for preparation of organic–inorganic hybrid materials [5]. Up to date, various metal complexes with one- (1D), two- (2D), or three-dimensional (3D) structures have been obtained by using this strategy [6]. However, the exploration of synthetic routes is a long-term challenge since the assembly reactions can be affected by factors like the nature of organic ligands, solvents, templates, counterions and so on [7]. Thus further research is required to achieve information for controlling and predicting the relevant structures as well as to establish the relationship between structures and properties.

On the other hand, crystal engineering of coordination frameworks based on multidentate ligands represents growing area of coordination and supramolecular chemistry. In particular, metal-organic architectures with flexible ligands attract more and more attention from chemists, since the flexible ligands can adopt varied conformation upon the different geometric requirement of the metal ions and lead to form diverse structures [8]. We focus our attention on the assembly of varied metal salts with flexible imidazole-containing tripodal ligands, for example 1,3,5-tris(imidazole-1-ylmethyl)-2,4,6-trimethylbenzene (TITMB), 1,3,5-tris(imidazole-1-ylmethyl)benzene (TIB), and metal complexes with various structures and properties have been obtained [9–13]. As an extension of our work, we synthesized flexible tripodal ligands with pyridyl groups, namely 1,3,5-tris(2-pyridylmethoxyl)benzene ($L_2$) and 1,3,5-tris(3-pyridylmethoxyl)benzene ($L_3$) as shown in Scheme 1 [8]. Herein we report five new metal complexes $[Ag_2(L_2)_2](BF_4)_2 \cdot CH_3CN \cdot CH_3OH$ (**1**), $[Ag(L_2)(CF_3SO_3)]$ (**2**), $[Ag(L_3)]ClO_4 \cdot CH_3OH$ (**3**), $[Ag_2(L_3)_2](CF_3SO_3)_2 \cdot CH_3CN \cdot CH_3OH \cdot H_2O$ (**4**) and $[Ag(L_3)]PF_6 \cdot 2CH_3CN$ (**5**) synthesized by reactions of $L_2$ or $L_3$ with the corresponding Ag(I) salts, respectively. The complexes were characterized by single crystal X-ray diffraction analyses, and their photoluminescence and anion-exchange properties were investigated.

* Corresponding author. Fax: +86 25 8331 4502.
*E-mail address:* sunwy@nju.edu.cn (W.-Y. Sun).

0022-4596/$ - see front matter © 2010 Elsevier Inc. All rights reserved.
doi:10.1016/j.jssc.2010.07.036

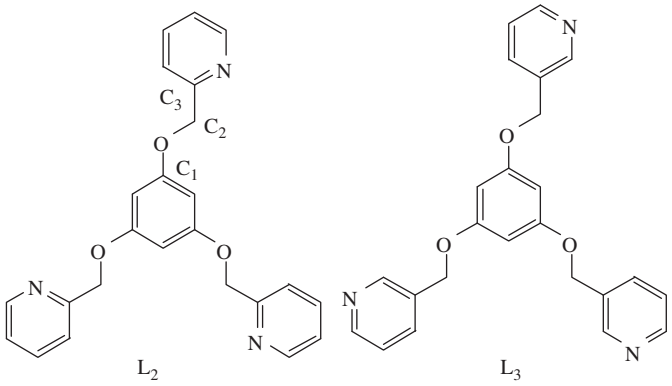


**Scheme 1.** Schematic structure of ligands $L_2$ and $L_3$.

## 2. Experimental section

### 2.1. Materials and measurements

All commercially available chemicals are of reagent grade and were used as received without further purification. Ligands $L_2$ and $L_3$ were prepared as reported previously [8]. Solvents of methanol ($CH_3OH$), acetonitrile ($CH_3CN$), etc. were purified according to the standard methods. All procedures for synthesis of Ag(I) complexes were carried out in the dark. C, H, N elemental analyses were performed on a Perkin-Elmer 240C Elemental Analyzer at the Analysis Center of Nanjing University. Infrared (IR) spectra were recorded on a Bruker Vector22 FT-IR Spectrophotometer by using KBr pellets. The photoluminescent spectra for the powdered solid samples were recorded at room temperature on an Aminco Bowman Series 2 Spectrofluorometer with a xenon arc lamp as the light source and all the measurements were carried out under the same conditions.

### 2.2. Syntheses

#### 2.2.1. $[Ag_2(L_2)_2](BF_4)_2 \cdot CH_3CN \cdot CH_3OH$ (**1**)

A methanolic solution (10 mL) of $L_2$ (24.0 mg, 0.06 mmol) was slowly added with stirring to an acetonitrile solution (10 mL) of $AgBF_4$ (11.7 mg, 0.06 mmol). The mixture was stirred for 15 min and was filtrated out. The clear filtrate stood at ambient temperature for several weeks, and single crystals suitable for X-ray diffraction analyses were obtained by slow evaporation of the filtrate. Yield: 48%. Anal. calcd. for $C_{51}H_{49}B_2Ag_2F_8N_7O_7$: C, 48.56; H, 3.92; N, 7.77%. Found: C, 48.64; H, 3.84; N, 7.69%. FT-IR (KBr: $cm^{-1}$): 1600(s), 1572(m), 1484(m), 1437(m), 1172(s), 1152(s), 1058(s), 1008(m), 818(m), 806(m), 766(m).

#### 2.2.2. $[Ag(L_2)(CF_3SO_3)]$ (**2**)

The procedure for preparation of complex **2** is the same as that for **1** except for $AgBF_4$ replaced by $AgCF_3SO_3$ (15.4 mg, 0.06 mmol). Yield: 38%. Anal. calcd. for $C_{25}H_{21}AgF_3N_3O_6S$: C, 45.75; H, 3.23; N, 6.40%. Found: C, 45.68; H, 3.14; N, 6.31%. FT-IR (KBr: $cm^{-1}$): 1602(s), 1479(m), 1438(m), 1376(m), 1251(s), 1169(s), 1069(m), 1035(m), 816(m), 760(m), 706(m).

#### 2.2.3. $[Ag(L_3)]ClO_4 \cdot CH_3OH$ (**3**)

The title complex was also prepared by the same method as that for preparation of complex **1** using $L_3$ (24.0 mg, 0.06 mmol) in methanol solution (10 mL) and $AgClO_4$ (13.1 mg, 0.06 mmol) in acetonitrile solution (10 mL). Block crystals were obtained by slow evaporation of the filtrate in 49% yield. Anal. calcd. for $C_{25}H_{25}AgClN_3O_8$: C 47.01; H 3.95; N 6.58%. Found: C 47.08; H 3.99; N 6.48%. FT-IR (KBr: $cm^{-1}$): 1608(s), 1586(m), 1483(m), 1431(m), 1165(s), 1117(m), 1078(s), 806(m), 709(m).

#### 2.2.4. $[Ag_2(L_3)_2](CF_3SO_3)_2 \cdot CH_3CN \cdot CH_3OH \cdot H_2O$ (**4**)

The same method was used to prepare complex **4** using $L_3$ (24.0 mg, 0.06 mmol) in methanol solution (10 mL) and $AgCF_3SO_3$ (15.4 mg, 0.06 mmol) in acetonitrile solution (10 mL). Yield: 44%. Anal. calcd. for $C_{53}H_{51}Ag_2F_6N_7O_{14}S_2$: C, 45.35; H, 3.66; N, 6.98%. Found: C, 45.42; H, 3.70; N, 6.91%. FT-IR (KBr: $cm^{-1}$): 1603(s), 1458(m), 1431(m), 1264(s), 1166(s), 1071(m), 1032(m), 796(m), 706(m).

#### 2.2.5. $[Ag(L_3)]PF_6 \cdot 2CH_3CN$ (**5**)

When $AgNO_3$ (10.2 mg, 0.06 mmol) and $KPF_6$ (10.4 mg, 0.06 mmol) were used instead of $AgCF_3SO_3$ (15.4 mg, 0.06 mmol) in preparation of **4**, colorless block crystals were obtained after about 2 weeks. Yield: 61%. Anal. calcd. for $C_{28}H_{27}AgF_6N_5O_3P$: C 45.79; H 3.71; N 9.54%. Found: C 45.88; H 3.78; N 9.48%. IR (KBr, $cm^{-1}$): 1604(s), 1434(m), 1158(s), 1051(m), 843(s), 704(m).

**Safety note**: Perchlorate salts of metal complex with organic ligands are potentially explosive and should be handled with care.

### 2.3. Crystal structure determination

The crystallographic data collections for complexes **1**–**5** were carried out on a Rigaku RAXIS-RAPID Imaging Plate diffractometer at 200 K, using graphite-monochromated Mo-$K\alpha$ radiation ($\lambda$=0.71075 Å). The structures were solved by direct methods with SIR92 [14], and expanded using Fourier technique [15]. All non-hydrogen atoms were refined anisotropically by the full-matrix least-squares method. The hydrogen atoms except for those of water molecules were generated geometrically and the ones of water molecule in **4** were located directly. All calculations were carried out on SGI workstation using the teXsan crystallographic software package of Molecular Structure Corporation [16]. In complex **1**, the F1, F2, F3, F4 atoms disordered into two positions with site occupation factors of 0.54(2) and 0.46(2), while the F8 and B2 atoms disordered into two positions with site occupation factors of 0.741(4) and 0.259(4), respectively. In complex **4**, S1, F3, O13, C10 disordered into two positions with site occupation factors of 0.606(6) and 0.394(6) and S2, F4, F5, F6, O21, O22, O23 and C20 disordered into two positions with site occupation factors of 0.501(5) and 0.499(5), respectively. Details of the crystal parameters, data collection and refinements for complexes **1**–**5** are summarized in Table 1, and selected bond lengths and angles with their estimated standard deviations are listed in Table 2. Hydrogen bonding data of the complexes are summarized in Table 3.

### 2.4. Anion-exchange of complexes **3** and **5**

The powder sample (50.0 mg) of **3** or **5** was suspended in water (10 mL), and then $NaNO_3$ (1.0 g) was added. The mixture was stirred for 36 h at ambient temperature, then was filtered, washed with deionized water three times, and dried to give the exchanged product of **3A** and **5A**, respectively. Elemental analysis for **3A**: C, 49.01; H, 4.05; N, 9.37%; calcd. for $[Ag(L_3)]NO_3 \cdot H_2O$ ($C_{24}H_{23}N_4O_7Ag$): C, 49.08; H, 3.95; N, 9.54%; for **5A**: C, 49.11; H, 3.97; N, 9.45%; calcd. for $[Ag(L_3)]NO_3 \cdot H_2O$ ($C_{24}H_{23}N_4O_7Ag$): C, 49.08; H, 3.95; N, 9.54%. The powder sample of **3A** (50.0 mg) was suspended in water (10 mL), and then $NaClO_4$ (1.0 g) was added. The mixture was stirred for 36 h at ambient temperature, then filtered, washed with deionized water three times, and dried to give the exchanged product of **3B**. Elemental analysis for **3B**: C, 46.17; H, 3.73; N, 6.89%; calcd. for $[Ag(L_3)]ClO_4 \cdot H_2O$ ($C_{24}H_{23}N_3O_8ClAg$): C,

**Table 1**
Crystallographic data for complexes **1**–**5**.

| | **1** | **2** |
|---|---|---|
| Empirical formula | $C_{51}H_{49}B_2Ag_2F_8N_7O_7$ | $C_{25}H_{21}AgF_3N_3O_6S$ |
| Formula weight | 1261.33 | 656.38 |
| Temperature (K) | 200 | 200 |
| Crystal system | Monoclinic | Monoclinic |
| Space group | $P2_1/c$ | $P2_1/c$ |
| Crystal size (mm) | $0.20\times0.20\times0.01$ | $0.30\times0.30\times0.04$ |
| $a$ (Å) | 14.3728(3) | 15.230(9) |
| $b$ (Å) | 12.9250(3) | 9.091(7) |
| $c$ (Å) | 30.3665(5) | 18.952(10) |
| $\beta$ (°) | 106.688(1) | 101.841(17) |
| $V$ (Å$^3$) | 5403.55(19) | 2568(3) |
| $Z$ | 4 | 4 |
| $\lambda$ (Å) | 0.71075 | 0.71075 |
| $D_c$ (g cm$^{-3}$) | 1.550 | 1.698 |
| $\mu$ (Mo $K\alpha$) (cm$^{-1}$) | 0.809 | 0.935 |
| Independent reflns. | 12331 | 5849 |
| $R_{int}$ | 0.0748 | 0.0406 |
| Observed reflns. | 4642 | 3830 |
| $R_1$[a] ($I>2\sigma(I)$) | 0.0406 | 0.0275 |
| w$R_2$[b] ($I>2\sigma(I)$) | 0.0394 | 0.0419 |

| | **3** | **4** | **5** |
|---|---|---|---|
| Empirical formula | $C_{25}H_{25}AgClN_3O_8$ | $C_{26.5}H_{25.5}AgF_3N_{3.5}O_7S$ | $C_{28}H_{27}AgF_6N_5O_3P$ |
| Formula weight | 638.80 | 701.93 | 734.39 |
| Temperature (K) | 200 | 200 | 200 |
| Crystal system | Orthorhombic | Monoclinic | Orthorhombic |
| Space group | $Pna2_1$ | $Cc$ | $Pna2_1$ |
| Crystal size (mm) | $0.15\times0.15\times0.15$ | $0.30\times0.10\times0.07$ | $0.25\times0.15\times0.10$ |
| $a$ (Å) | 22.258(15) | 27.999(3) | 7.0461(11) |
| $b$ (Å) | 11.154(9) | 15.9739(14) | 26.607(4) |
| $c$ (Å) | 10.409(9) | 14.4213(16) | 16.224(2) |
| $\beta$ (°) | 90.00 | 115.391(7) | 90.00 |
| $V$ (Å$^3$) | 2584(3) | 5826.9(10) | 3041.5(7) |
| $Z$ | 4 | 8 | 4 |
| $\lambda$ (Å) | 0.71075 | 0.71075 | 0.71075 |
| $D_c$ (g cm$^{-3}$) | 1.642 | 1.600 | 1.604 |
| $\mu$ (Mo $K\alpha$) (cm$^{-1}$) | 0.938 | 0.832 | 0.791 |
| Independent reflns. | 5865 | 11835 | 6929 |
| $R_{int}$ | 0.0508 | 0.0559 | 0.0897 |
| Observed reflns | 3374 | 6787 | 3455 |
| $R_1$[a] ($I>2\sigma(I)$) | 0.0351 | 0.0450 | 0.0422 |
| w$R_2$[b] ($I>2\sigma$ ($I$)) | 0.0636 | 0.0829 | 0.0481 |

[a] $R_1=\sum||F_o|-|F_c||/\sum|F_o|$.
[b] $wR_2=|\sum w(|F_o|^2-|F_c|^2)|/\sum|w(F_o)^2|^{1/2}$, where $w=1/[\sigma^2(F_o^2)+(aP)^2+bP]$. $P=(F_o^2+2F_c^2)/3$.

46.14; H, 3.71; N, 6.73%. The powder sample of 5A (50.0 mg) was suspended in water (10 mL), and then $NaPF_6$ (1.0 g) was added. The mixture was stirred for 36 h at ambient temperature, then filtered, washed with deionized water three times, and dried to give the exchanged product of **5B**. Elemental analysis for **5B**: C, 42.97; H, 3.43; N, 6.39%; calcd. for $[Ag(L_3)]PF_6\cdot H_2O$ ($C_{24}H_{23}N_3O_4PF_6Ag$): C, 43.01; H, 3.46; N, 6.27%.

## 3. Results and discussion

### 3.1. Crystal structure of complexes *1* and *2*

The results of crystallographic analysis indicate that complexes **1** and **2** have similar framework structure, accordingly only

**Table 2**
Selected bond lengths (Å) and bond angles (°) for complexes **1**–**5**.[a]

| | | | |
|---|---|---|---|
| **1** | | | |
| Ag1–N151 | 2.267(3) | Ag1–N11 | 2.286(3) |
| Ag1–N31#1 | 2.303(3) | Ag2–N131#2 | 2.20(3) |
| Ag2–N51 | 2.284(3) | Ag2–N111 | 2.291(3) |
| N151–Ag1–N11 | 125.64(11) | N151–Ag1–N31#1 | 121.53(10) |
| N11–Ag1–N31#1 | 112.52(11) | N131#2–Ag2–N51 | 121.18(10) |
| N131#2–Ag2–N111 | 116.27(10) | N51–Ag2–N111 | 122.55(11) |
| **2** | | | |
| Ag1–N51#3 | 2.287(2) | Ag1–N11 | 2.3300(17) |
| Ag1–N31#4 | 2.345(2) | Ag1–O11 | 2.5436(18) |
| N51#3–Ag1–N11 | 126.21(6) | N51#3–Ag1–N31#4 | 119.24(6) |
| N11–Ag1–N31#4 | 98.40(6) | N51#3–Ag1–O11 | 100.98(5) |
| N11–Ag1–O11 | 103.22(7) | N31#4–Ag1–O11 | 106.70(6) |
| **3** | | | |
| Ag1–N11 | 2.199(4) | Ag1–N31#5 | 2.206(4) |
| Ag1–N51#6 | 2.334(4) | | |
| N11–Ag1–N31#5 | 139.42(14) | N11–Ag1–N51#6 | 108.99(15) |
| N31#5–Ag1–N51#6 | 109.36(16) | | |
| **4** | | | |
| Ag1–N51#7 | 2.274(6) | Ag1–N31 | 2.299(4) |
| Ag1–N11 | 2.292(6) | Ag2–N151#8 | 2.266(5) |
| Ag2–N131#9 | 2.266(5) | Ag2–N111 | 2.302(5) |
| N51#7–Ag1–N31 | 118.8(2) | N51#7–Ag1–N11 | 118.90(18) |
| N31–Ag1–N11 | 118.0(2) | N151#8–Ag2–N131#9 | 118.00(19) |
| N111–Ag2–N151#8 | 117.8(2) | N131#9–Ag2–N111 | 118.16(19) |
| **5** | | | |
| Ag1–N51#10 | 2.234(4) | Ag1–N31#11 | 2.259(3) |
| Ag1–N11 | 2.267(3) | | |
| N51#10–Ag1–N31#11 | 123.09(14) | N51#10–Ag1–N11 | 119.82(14) |
| N31#11–Ag1–N11 | 114.98(14) | | |

[a] Symmetry transformations used to generate equivalent atoms: #1: $-x, y-1/2, -z+3/2$; #2: $-x+1, y+1/2, -z+3/2$; #3: $x, -y+1/2, z+1/2$; #4: $-x+2, y+1/2, -z+3/2$; #5: $-x+3/2, y-1/2, z-3/2$; #6: $x-1/2, -y+1/2, z-1$; #7: $x+1/2, y-1/2, z$; #8: $x-1/2, y+1/2, z$; #9: $x-1/2, y-1/2, z$; #10: $-x+3/2, y-1/2, z-1/2$; #11: $-x+3/2, y-1/2, z+1/2$.

**Table 3**
Hydrogen bonding data for complexes **1**, **4** and **5**.

| D–H···A | D···A (Å) | D–H–A (deg.) |
|---|---|---|
| **1** | | |
| C11–H5···F4#1 | 3.355(14) | 142 |
| O201–H49···F2#1 | 3.10(2) | 163 |
| C34–H13···F4 | 3.053(12) | 126 |
| C35–H14···F7#2 | 3.322(5) | 149 |
| C51–H17···O103#3 | 3.239(4) | 150 |
| C53–H18···F6#3 | 3.330(4) | 155 |
| C56–H21···F7 | 3.436(4) | 160 |
| C111–H25···F6 | 3.482(4) | 158 |
| C131–H31···N1 | 3.427(5) | 145 |
| C156–H42···F3#1 | 3.294(12) | 135 |
| C151–H37···O3#4 | 3.285(4) | 148 |
| **4** | | |
| O201–H49···O12#5 | 2.829(11) | 171 |
| O202–H50···O201 | 2.930(15) | 167(11) |
| O202–H51···O22#6 | 2.611(16) | 177(16) |
| C51–H17···O21#5 | 3.439(16) | 152 |
| C56–H21···O11#7 | 3.348(9) | 138 |
| C102–H22···O21#6 | 3.373(15) | 156 |
| C116–H30···O12#8 | 3.288(10) | 141 |
| C203–H48···F4#9 | 3.237(18) | 143 |
| **5** | | |
| C16–H9···F2 | 3.248(6) | 159 |

Symmetry transformations used to generate equivalent atoms: #1: $x, 1/2+y, 3/2-z$; #2: $-1+x, y, z$; #3: $1-x, 1/2+y, 3/2-z$; #4: $-x, -1/2+y, 3/2-z$; #5: $-1/2+x, 1/2+y, z$; #6: $x, 1-y, 1/2+z$; #7: $-1/2+x, 3/2-y, 1/2+z$; #8: $-1/2+x, 1/2-y, 1/2+z$; #9: $x, -y, 1/2+z$.

the structure of **1** is described here in detail, while the one of **2** is provided in supporting information (Fig. S1). In the cationic part of complex **1**, there are two independent Ag(I) and two $L_2$ ligands as shown in Fig. 1a. The Ag1 and Ag2 have similar coordination geometry and each Ag(I) atom is coordinated by three nitrogen atoms from three different $L_2$ ligands with Ag–N bond length varying from 2.267(3) to 2.303(3) Å and N–Ag–N bond angles ranging from 112.52(11) to 125.64(11)° as listed in Table 2. Thus the coordination geometry of each Ag(I) center in **1** can be regarded as triangle with N3 donor set. On the other hand, each $L_2$ acts as a three-connector linking three Ag(I) atoms to form a 2D network (Fig. 1b). It is noteworthy that there are two macrocycles in the 2D network, one is 24-membered $Ag_2(L_2)_2$ macrocyclic motif (A) with Ag · · · Ag separation of 10.37 Å and the other one is 48-membered $Ag_4(L_2)_4$ macrocycle (B) as shown in Fig. 1b. There are π–π interactions within the macrocycle A since the centroid-to-centroid separation is 3.79 Å and the dihedral angle between the two benzene ring planes is 0.8° (Fig. 1b) [17]. Each A ring is surrounded by four B rings, and in turn each B is surrounded by four A and four B rings. Therefore, the 2D network of **1** has $4.8^2$ topology as schematically shown in Fig. 1c, in which the $L_2$ ligand is represented by spoke radiating from a point (i.e. the centroid of benzene ring plane) and the Ag(I) center is represented by three-connecting node.

The crystal-packing diagram of **1** is shown in Fig. 1d. Tetrafluoroborate anions locate in the voids and are connected to the 2D layer through C–H···F hydrogen bonds with the C···F distances in the range from 3.053(12) to 3.482(4) Å, and the C–H–F angles varying from 126 to 160° as listed in Table 3. The solvent acetonitrile molecules are also held to the 2D layer by C131–H31···N1 hydrogen bond with a C···N distance of 3.427(5) Å. In addition, there are C–H···π interactions in complex **1** between the two pyridine rings from two adjacent layers [17], since the distance between the hydrogen atom bound to the carbon of a pyridine ring and the centroid of the other pyridine group in the adjacent layer is 2.97 Å (the distance between the carbon atom of the pyridine ring and the centroid of the other pyridine group in the adjacent layer is 3.70 Å), and the C–H–centroid angle is 135°. The 2D layers are held together by such C–H···π interactions to give a 3D structure (Fig. 1d).

In contrast to the three-coordinated Ag(I) in **1**, the Ag(I) in **2** is four-coordinated by three nitrogen atoms from three different $L_2$

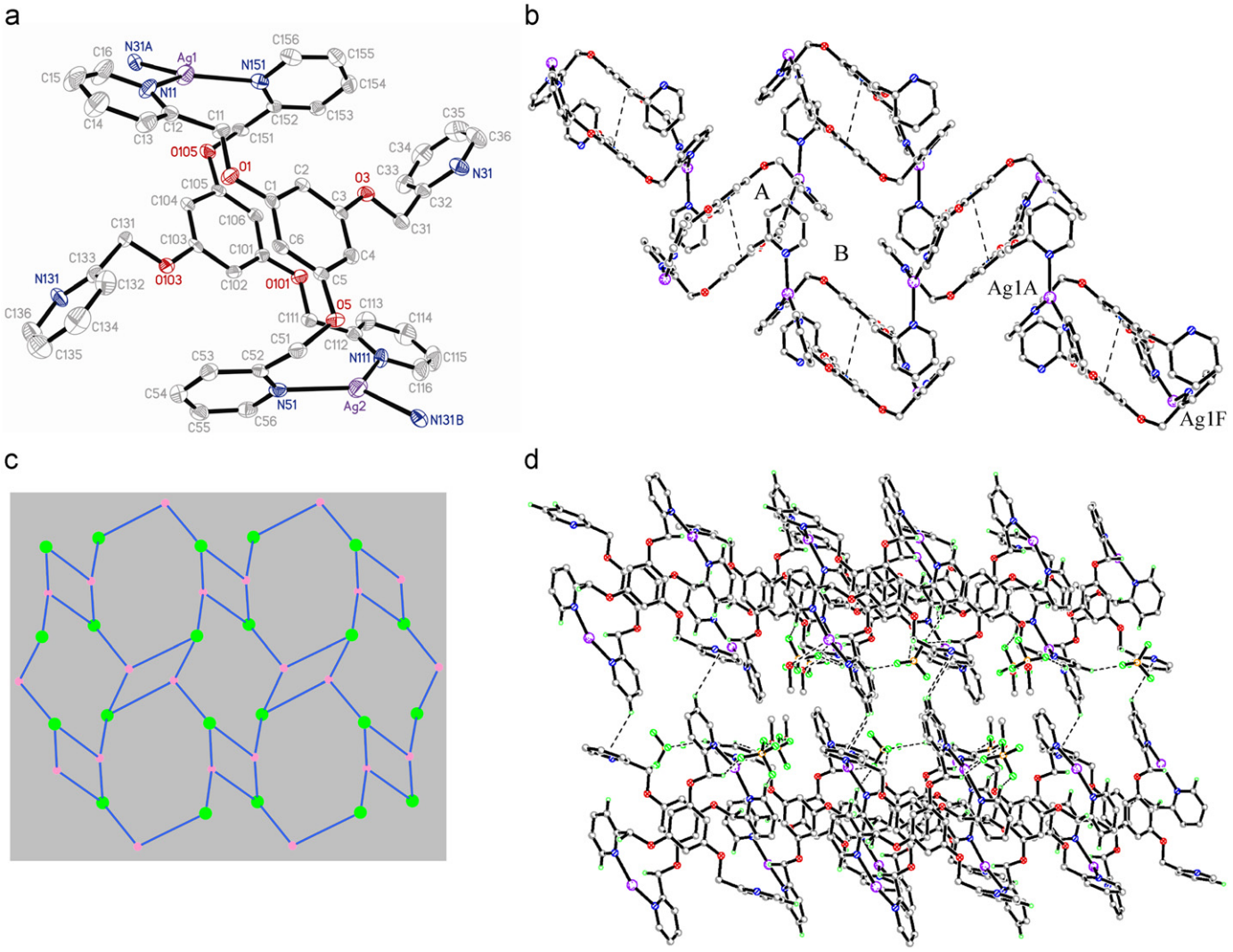


**Fig. 1.** (a) The coordination environment around the Ag(I) atoms in **1** with the ellipsoids drawn at 50% probability level, the $CH_3CN$, $CH_3OH$ molecules, $BF_4^-$ anions and hydrogen atoms are omitted for clarity. (b) 2D network structure of **1** with π–π interactions indicated by dashed lines. (c) Simplified $4,8^2$ topology of **1**, the small balls (pink) represent the centroids of the central benzene ring of $L_2$, the large ones (green) represent Ag(I) atoms. (d) Crystal-packing diagram of **1**, in which the hydrogen bonds and C–H···π interactions are indicated by dashed lines, $CH_3CN$ molecules are omitted for clarity (For interpretation of the references to color in this figure legend, the reader is referred to the web version of this article.).

ligands and one oxygen atom from $CF_3SO_3^-$ anion (Fig. S1a). A distance of 2.5436(18) Å between the Ag1 and O11 suggests the existence of Ag–O coordination [18,19]. The N–Ag–N angles are ranging from 98.40(6)° to 126.21(6)°, and the N–Ag–O ones are varying from 100.98(5)° to 106.70(6)° as listed in Table 2. Therefore, each Ag(I) atom in **2** has distorted tetrahedral coordination geometry. Nevertheless, complex **2** also has 2D network structure with $4.8^2$ topology (Fig. S1).

### 3.2. Crystal structure of complex *3*

When ligand $L_3$, instead of $L_2$, was used to react with different Ag(I) salts, complexes **3**–**5** were isolated. The X-ray crystallographic analysis revealed that complex **3** contains one silver(I), one ligand $L_3$, one perchlorate anion and one methanol molecule. The coordination environment of Ag(I) in complex **3** is displayed in Fig. 2a along with the atom-numbering scheme. It can be clearly seen that each Ag(I) atom in **3** is coordinated by three nitrogen atoms from three different $L_3$ ligands which is similar to the Ag(I) in **1**. Furthermore, each $L_3$ ligand also links three Ag(I) atoms like the $L_2$ in **1**, however, to generate a 3D structure with open channels occupied by non-coordinated $ClO_4^-$ anions and methanol molecules (Fig. 2b), rather than the 2D network observed in **1** as well as **2** (Figs. 1b and S1b).

The 3D framework of **3** can be regarded as a non-interpenetrated (10,3)-a net (Fig. 2c) by considering the metal center as three-connected node and the ligand as three-connector [18]. Five Ag(I) atoms and five $L_3$ ligands form a circuit of the (10,3)-a net (Fig. 2d) and helical unit in the (10,3)-a net can be found (Fig. 2e). It should be noticed that the most of previously reported (10,3)-a topological structures are interpenetrating nets [14]. Li et al. reported a non-interpenetrating (10,3)-a net by using bulky auxiliary triphenylphosphine ligand to avoid possible interpenetration [18]. Complex **3** provides an example of non-interpenetrated (10,3)-a topological net without bulky auxiliary ligand.

### 3.3. Crystal structure of complexes *4* and *5*

It is interesting to note that in contrast to the 3D structure of **3** with $ClO_4^-$ anion, complex **4** with $CF_3SO_3^-$ and **5** with $PF_6^-$ have similar 2D network structure. The coordination environment of Ag(I) atoms in **4** is shown in Fig. 3a with atom-numbering scheme.

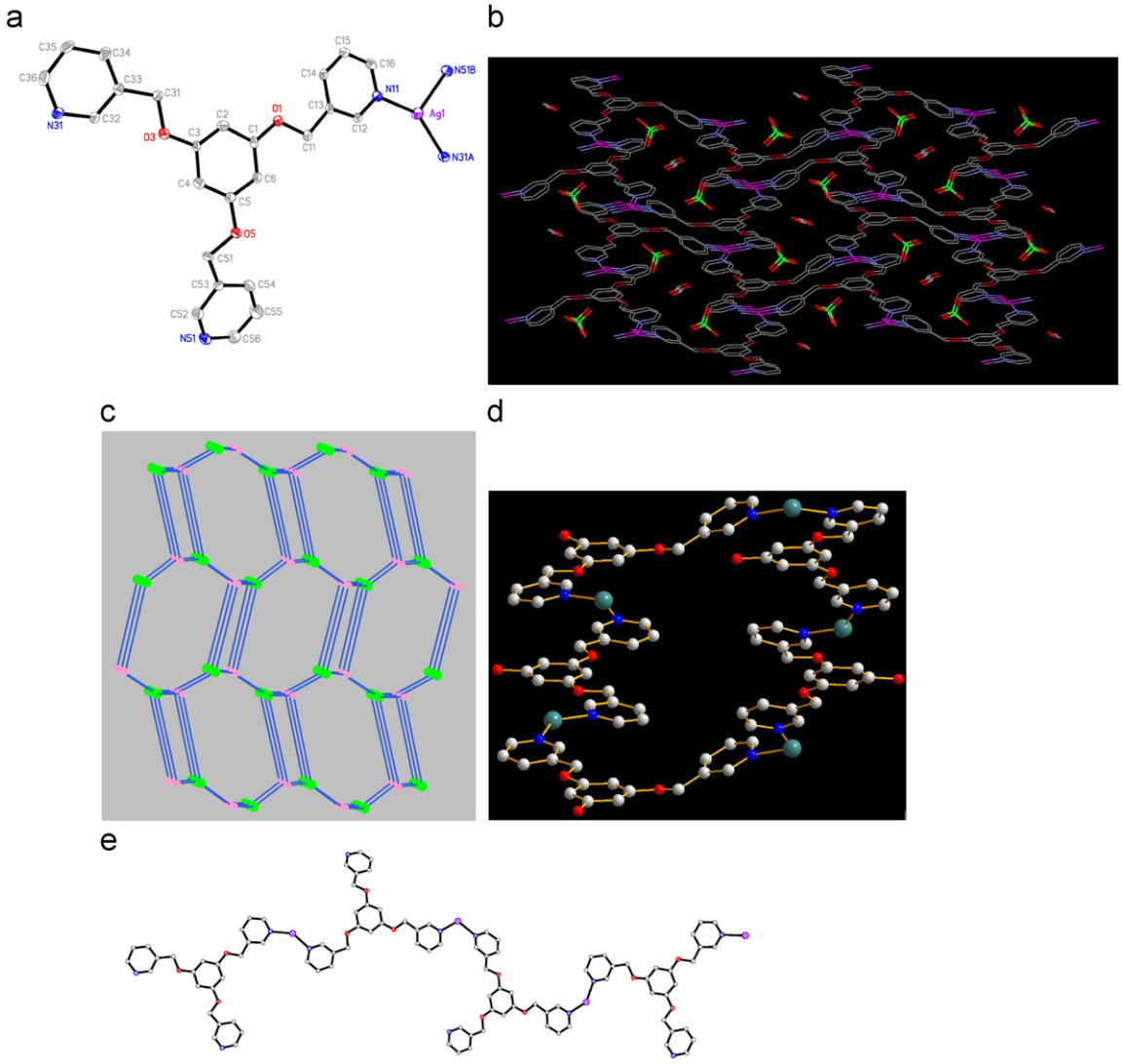


**Fig. 2.** (a) The coordination environment around the Ag(I) atom in **3** with the ellipsoids drawn at 50% probability level, the $ClO_4^-$, $CH_3OH$ molecule and hydrogen atoms are omitted for clarity. (b) 3D structure of complex **3**. (c) Simplified (10,3)-a topology of **3**, the small balls (pink) represent the centroids of the central benzene ring of $L_3$, the large ones (green) represent Ag(I) atoms. (d) A $M_5L_5$ macrocyclic ring in **3**. (e) Side view of the helix in **3** (For interpretation of the references to color in this figure legend, the reader is referred to the web version of this article.).

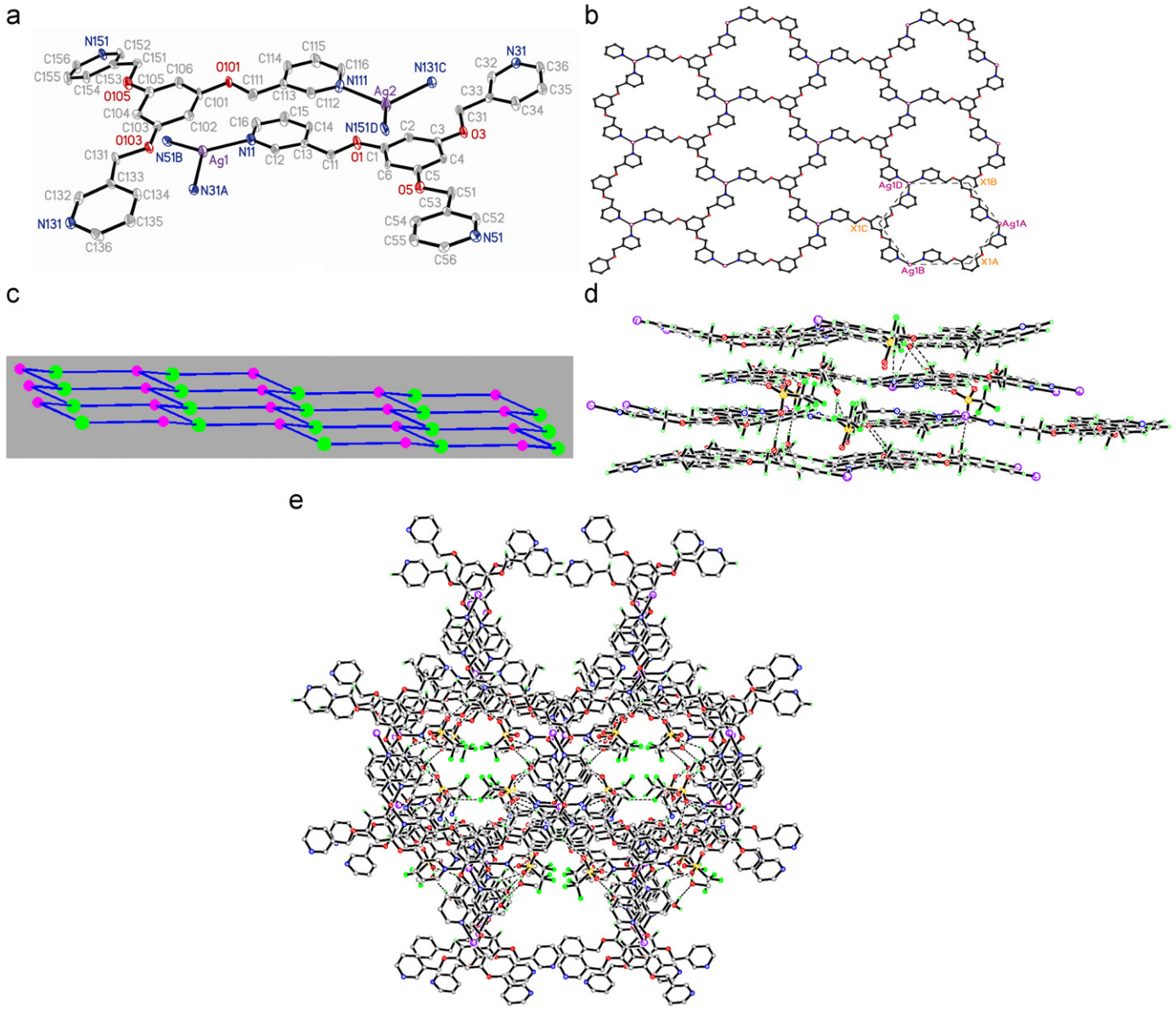


**Fig. 3.** (a) The coordination environment around the Ag(I) atoms in **4** with the ellipsoids drawn at 50% probability level, the $CF_3SO_3^-$ anion, $CH_3CN$, $CH_3OH$, water molecules and hydrogen atoms are omitted for clarity. (b) 2D network of **4** with Ag1 atoms. (c) Simplified (6,3) 2D network structure of **4**, the small balls (pink) represent the centroids of the central benzene ring of $L_3$, the large ones (green) represent Ag(I) atoms. Side (d) and top (e) views of crystal-packing diagram of **4**, hydrogen bonds are indicated by dashed lines (For interpretation of the references to color in this figure legend, the reader is referred to the web version of this article.)

There are two crystallographically independent cationic units each with one Ag(I) atom and one $L_3$ ligand. Each Ag(I) atom acts as a three-connected node and is coordinated by three nitrogen atoms from three individual $L_3$ ligands. On the other hand, each $L_3$ serves as a three-connector coordinating to three Ag(I) atoms. Each ligand $L_3$ using two of its three pyridyl groups connects two Ag(I) atoms to form a 42-membered $M_3(L_3)_3$ macrometallocyclic ring through Ag–N coordination bonds. The remarkable structural feature of complex **4** is that the $M_3(L_3)_3$ macrocyclic motifs extend to form a 2D network with (6,3) topology which can be clearly seen from Fig. 3b and c with centroid of benzene ring-Ag(I) separations of 9.35 (Ag1D···X1C=Ag1A···X1A), 9.29 (X1B···Ag1D=X1A···Ag1B), 9.34 Å (Ag1A···X1B=Ag1B···X1C) (Fig. 3b showing the Ag1-$L_3$ layer), while the corresponding ones in Ag2-$L_3$ network are 9.36, 9.28, 9.33 Å, respectively. It should be noticed that the $CF_3SO_3^-$ anion did not coordinate to the Ag(I) atom in **4**, which is different from that in **2**.

Fig. 3d and e shows the crystal-packing diagrams of complex **4**. It can be seen that there are open channels occupied by $CF_3SO_3^-$ anions and solvent molecules. The $CF_3SO_3^-$ anions link two 2D layers together through the C–H···O hydrogen bonds. There are O–H···O hydrogen bonds between the methanol and water molecules and also between the water molecule and the $CF_3SO_3^-$ anion (Table 3, Fig. 3d). In addition, there are π–π interactions between two pyridine ring planes from adjacent layers with a centroid-to-centroid separation of 3.97 Å and a dihedral angle of 2.7°, and between the pyridine ring and benzene ring with a centroid-to-centroid distance of 3.65 Å and a dihedral angle of 16.9°. Therefore, the hydrogen bonding and π–π interactions play important role in the stabilizing the structure of complex **4**.

The asymmetric unit of complex **5** contains one $L_3$ ligand, one Ag(I), one $PF_6^-$ and two $CH_3CN$ molecules. In the cationic part of **5**, each Ag(I) links three $L_3$ ligands and each $L_3$ ligand in turn

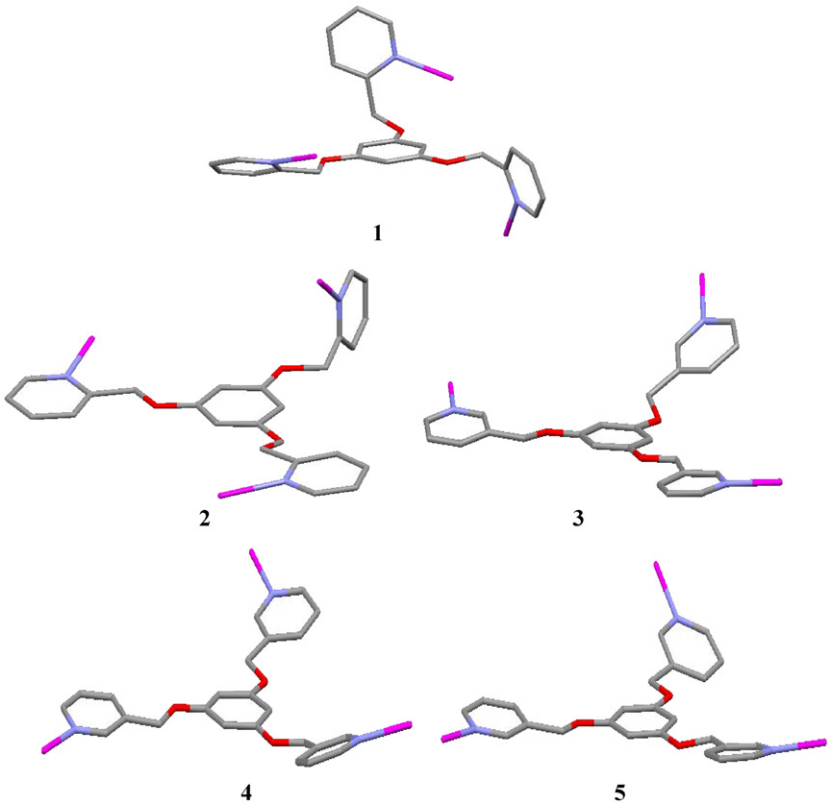


**Scheme 2.** Typical conformations of ligands in complexes **1**–**5** (only one of two similar conformations is shown for **1** and **4**).

**Table 4**
Conformational parameters for complexes **1**–**5**.

| Complex | $\varphi$1 (deg.)[a] | $\varphi$1 (deg.) | $\varphi$1 (deg.) | $\varphi$2 (deg.)[b] | $\varphi$2 (deg.) | $\varphi$2 (deg.) |
|---|---|---|---|---|---|---|
| **1** | 33.5 | 77.9 | 86.6 | 9.4 | 6.7 | 73.1 |
| **1** | 28.7 | 78.9 | 86.1 | 8.3 | 6.8 | 73.8 |
| **2** | 2.5 | 94.8 | 2.5 | 0.3 | 12.3 | 9.6 |
| **3** | 6.0 | 7.9 | 24.5 | 2.2 | 1.7 | 30.4 |
| **4** | 4.3 | 19.8 | 13.8 | 12.8 | 14.9 | 2.0 |
| **4** | 5.5 | 18.6 | 6.4 | 3.3 | 14.5 | 5.1 |
| **5** | 21.8 | 10.0 | 6.3 | 5.8 | 9.0 | 5.8 |

[a] $\varphi$1 refers to the dihedral angle between the pyridyl ring and central benzene ring planes.
[b] $\varphi$2 refers to the torsion angle defined by C1–O–C2–C3, where C1, C2 and C3 are labeled in Scheme 1.

connects three Ag(I) atoms to give 2D network structure with (6,3) topology (Fig. S2), which is similar to that in **4**. The 2D layers repeat in an ···ABAB··· stacking sequence with open channels occupied by $PF_6^-$ anions, which link the framework through C16–H9···F2 hydrogen bond together with $\pi$–$\pi$ interactions to form 3D framework structure of **5** (Fig. S2).

### 3.4. Comparison of the structures

Complexes **1** and **2** with $L_2$ ligand show similar 2D network structure with the same $4.8^2$ topology, indicating that the counteranions are not relevant to the framework structure of the complexes. However, in the case of complexes with $L_3$ ligand, **3** with perchlorate anion has 3D structure with (10,3)-a topology while **4** with $CF_3SO_3^-$ and 5 with $PF_6^-$ are 2D networks with (6,3) topology. The results imply that the counteranions are subtle in the assembly of metal complexes. The difference between **1**–**2** and **3**–**5** are apparently caused by the different structure of ligands $L_2$ and $L_3$.

It is noteworthy that the connection modes of Ag(I) and ligands are the same in complexes **1**–**5**, namely each Ag(I) coordinates with three ligands and each ligand connects three Ag(I) atoms, however, the flexible ligands $L_2$ and $L_3$ show different conformations in these complexes as illustrated in Scheme 2. To elucidate the conformation of each ligand, dihedral angles between the pyridyl ring and central benzene ring plane ($\varphi$1) and the torsion angles of C1–O–C2–C3 ($\varphi$2) as labeled in Scheme 1 are defined and the calculated values are listed in Table 4. A value of $\varphi$1 close to zero or 180° implies that the pyridyl ring is close to parallel with the central benzene ring plane, and a near 90° value of $\varphi$1 indicates the near perpendicular relationship between the pyridyl ring and the central benzene ring. On the other hand, when the value of $\varphi$2 is close to zero or 180°, it means that the flexible arm is extended to the central benzene ring plane, otherwise, when the value of $\varphi$2 is close to 90°, the arm locates above or below the central benzene ring plane [14]. According to the $\varphi$1 and $\varphi$2 values listed in Table 4, it is clear that the flexible ligands $L_2$ and $L_3$ adopt different conformations in complexes **1–5** (Scheme 2). In **1** the Ag(I) is three-coordinated, while in **2** the Ag(I) is four-coordinated and the ligand $L_2$ has different conformation from that in **1**. The results show that the flexible ligand can adjust its conformation to meet the geometric requirement of the metal ion. In the case of complexes **3**–**5**, all the small values of φ1 and φ2 of ligand $L_3$ indicate that the ligands in these complexes have extended conformation, however, their subtle difference in conformation is responsible for the formation of 3D structure of **3** and 2D network structures of **4** and **5**.

### 3.5. Luminescence properties of the complexes

The inorganic–organic hybrid coordination polymers with $d^{10}$ metal have been investigated for photoluminescence properties and potential applications as light-emitting diodes [20]. The photoluminescent properties of complexes **1**–**5** were studied in the solid state at room temperature. The emission spectra of **1**–**5** under the same excitation wavelength of 352 nm are shown in Fig. 4. Ligands $L_2$ and $L_3$ showed broad emission around 425 and 420 nm under the same excitation wavelength, respectively [8]. The maximum emission wavelengths of complexes **1** and **2** are 428 and 422 nm, respectively, which are close to that of ligand $L_2$. While the emissions observed in complexes **3**, **4**, **5** are at 390, 410, 394 nm with 10–30 nm blue-shifts compared with that of ligand $L_3$. The emissions observed in the complexes **1**–**5** may be tentatively assigned to the $\pi$–$\pi^*$ intraligand photoluminescence due to their resemblance of the emission bands as discussed previously, and the observed shifts of the emission maximum between the Ag(I) complexes and the corresponding ligand are considered to mainly originate from the coordination interactions between the metal atoms and the ligands [8,21–25]. In addition, in contrast to the weak or unobservable luminescence of silver(I) complexes at room temperature [7a], complexes **1**–**5** show apparent photoluminescence at ambient temperature implying that they may be good candidates for potential photoactive material.

### 3.6. Anion-exchange properties of complexes *3* and *5*

As revealed by the crystal structure analysis of the complexes, the anions locate within the channels of framework and held there through hydrogen bonding interactions except for complex **2** where the $CF_3SO_3^-$ anions coordinate to the Ag(I) atoms. The complexes are insoluble in water, and the anion-exchange properties of **3** with 3D structure and **5** with 2D layer structure were investigated. The FT-IR spectra of the exchanged solid **3A** and the as-synthesized **3** are shown in Fig. 5a and b, respectively. Intense band at 1384 $cm^{-1}$ appeared, which is from the $NO_3^-$ vibration, while the intense bands from 1120 to 1091 $cm^{-1}$ of the $ClO_4^-$ anion disappeared in the spectrum of **3A** (Fig. 5b). Furthermore, the results of elemental analysis of the anion exchanged product **3A** (see experimental section) also suggest the complete anion exchange.

To investigate the reversibility of this anion-exchange process, the excess $NaClO_4$ was added to the suspension mixture of the **3A**

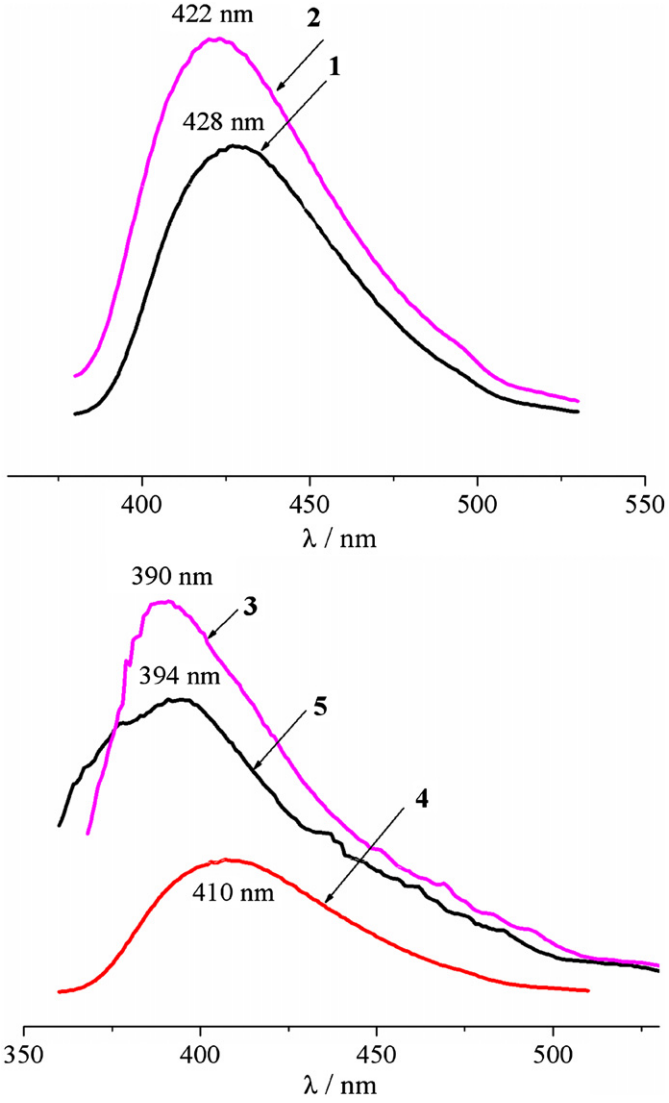


**Fig. 4.** Photoluminescent emission spectra of complexes **1**–**5** in the solid state.

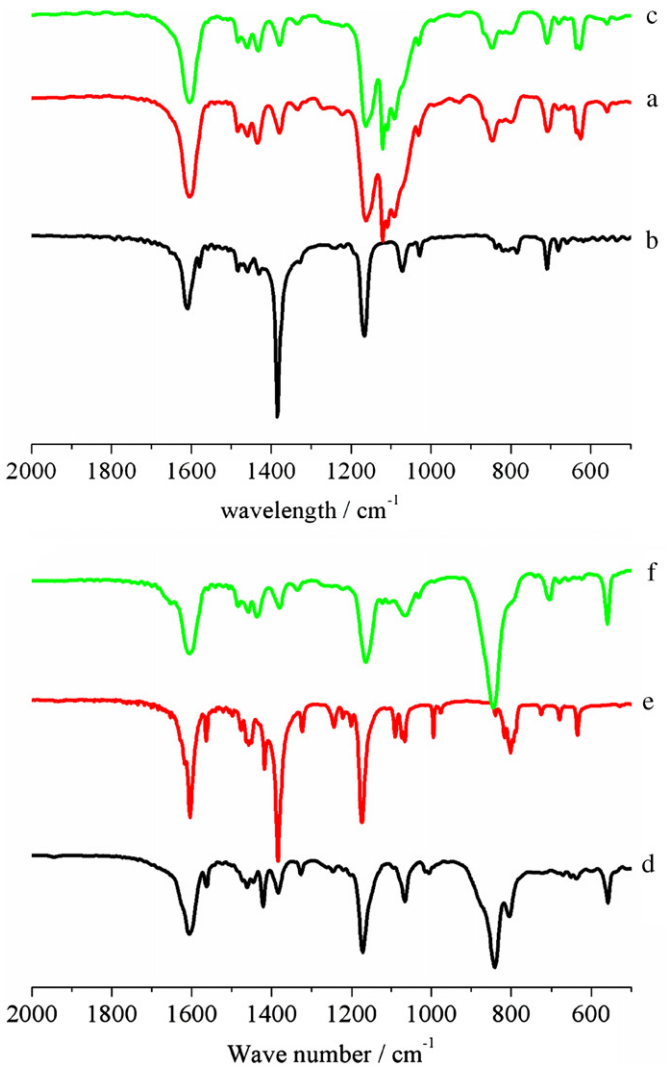


**Fig. 5.** FT-IR spectra of (a) complex **3**, (b) complex **3A**, (c) complex **3B**. FT-IR spectra of (d) complex **5**, (e) complex **5A**, (f) complex **5B**.

in water and the FT-IR spectrum of the exchanged solid **3B** shows that the intense band of $NO_3^-$ disappeared while the intense bands of $ClO_4^-$ appeared (Fig. 5c), implying the complete anion exchange, which is also supported by the results of elemental analysis. The results indicate that complex **3** has reversible anion-exchange property.

The anions exchange properties of complex **5** are also explored. The IR spectral (Fig. 5d–f) and elemental data reveal that the $PF_6^-$ anions in complex **5** can be exchanged reversibly by $NO_3^-$.

The results indicate that the anions hydrogen bonded to the 3D framework in **3** and to the 2D network in **5** can be exchanged reversibly as previously reported for the 2D and 3D frameworks with imidazole-containing ligands [7f,7g,26]. It is worthy to note that such anion exchange is also an anion recognition process as reported for the complex $[Zn(bib)_2(H_2O)_2](NO_3)_2 \cdot 2H_2O$ [bib= 1-bromo-3,5-bis(imidazol-1-ylmethyl)benzene] [26a]. The anion exchanges occurred reversibly between $NO_3^-$ and $ClO_4^-$ in **3** and between $NO_3^-$ and $PF_6^-$ in **5** indicate that the vacancies in the frameworks **3** and **5** are large enough to allow the anions exchanged reversibly in these complexes.

## 4. Conclusions

Flexible tripodal ligands with 2- and 3-pyridyl groups were used to react with different Ag(I) salts and complexes with 2D and 3D structures and ($4.8^2$), (10,3)-a and (6,3) topologies were obtained. The results show that the flexible ligand can have different conformation to meet geometric requirement of metal atom. The present study further suggests that the ligands as well as the counteranions have subtle but important influence on the structure of the complexes.

## Acknowledgments

This work was financially supported by the National Natural Science Foundation of China (Grant nos. 20731004 and 20721002), the National Basic Research Program of China (Grant nos. 2007CB925103 and 2010CB923303).

## Appendix A. Supporting information

Supplementary data associated with this article can be found in the online version at doi:10.1016/j.jssc.2010.07.036.

## References

[1] [a] Y.Q. Xu, D.Q. Yuan, B.L. Wu, L. Han, M.Y. Wu, F.L. Jiang, M.C. Hong, Cryst. Growth Des. 6 (2006) 1168;
[b] F.P. Huang, J.L. Tian, W. Gu, X. Liu, S.P. Yan, D.Z. Liao, P. Cheng, Cryst. Growth Des. 10 (2010) 1145.
[2] [a] X.Q. Song, Z.P. Zang, W.S. Liu, Y.J. Zhang, J. Solid State Chem. 182 (2009) 841;
[b] H.J. Mo, Y.R. Zhong, M.L. Cao, Y.C. Ou, B.H. Ye, Cryst. Growth Des. 9 (2009) 488.
[3] [a] W.P. Su, M.C. Hong, J.B. Weng, Y.C. Liang, Y.J. Zhao, R. Cao, Z.Y. Zhou, A.S.C. Chan, Inorg. Chim. Acta 331 (2002) 8;
[b] T.J. Burchell, D.J. Eisler, R.J. Puddephatt, Inorg. Chem. 43 (2004) 5550;
[c] R. Peng, D. Li, T. Wu, X.P. Zhou, S.W. Ng, Inorg. Chem. 46 (2006) 4035;
[d] J.C. Dai, X.T. Wu, S.M. Hu, Z.Y Fu, J.J. Zhang, W.X. Du, H.H. Zhang, R.Q. Sun, Eur. J. Inorg. Chem. (2004) 2096.
[4] [a] L. Raehm, L. Mimassi, C. Guyard-Duhayon, H. Amouri, M.N. Rager, Inorg. Chem. 42 (2003) 5654;
[b] D.B. Mitzi, J. Chem. Soc., Dalton Trans. (2001) 1;
[c] B.H. Ye, M.L. Tong, X.M. Chen, Coord. Chem. Rev. 249 (2005) 545;
[d] J. Wang, Z.J. Lin, Y.C. Ou, N.L. Yang, Y.L. Zhang, M.L. Tong, Inorg. Chem. 47 (2008) 190;
[e] X.D. Chen, H.F. Wu, X.H. Zhao, X.J. Zhao, M. Du, Cryst. Growth Des. 7 (2007) 124;
[f] J.L.C. Rowsell, O.M. Yaghi, J. Am. Chem. Soc. 128 (2006) 1304;
[g] S. Kitagawa, R. Kitaura, S. Noro, Angew Chem. Int. Ed. 43 (2004) 2334;
[h] L.Y. Kong, H.F. Zhu, Y.Q. Huang, T. Okamura, X.H. Lu, Y. Song, G.X. Liu, W.Y. Sun, N. Ueyama, Inorg. Chem. 45 (2006) 8098.
[5] G. Ferey, Chem. Mater. 13 (2001) 3084.
[6] [a] M.L. Tong, X.M. Chen, X.L. Yu, T.C.W. Mak, J. Chem. Soc., Dalton Trans. (1998) 5;
[b] M.A. Withersby, A.J. Blake, N.R. Champness, P. Hubberstey, W.S. Li, M. Schröder, Angew. Chem. Int. Ed. 36 (1997) 2327.
[7] [a] M.L. Tong, X.M. Chen, B.H. Ye, L.N. Ji, Angew. Chem. Int. Ed. 38 (1999) 2237;
[b] B.L. Fei, W.Y. Sun, K.B. Yu, W.X. Tang, J. Chem. Soc., Dalton Trans. (2000) 805;
[c] H.F. Zhu, W. Zhao, T.-a. Okamura, J. Fan, W.Y. Sun, N. Ueyama, New J. Chem. 28 (2004) 1010;
[d] J. Fan, L. Gan, H. Kawaguchi, W.Y. Sun, K.B. Yu, W.X. Tang, Chem. Eur. J. 9 (2003) 3965;
[e] W. Zhao, J. Fan, T.-a. Okamura, W.Y. Sun, N. Ueyama, New J. Chem. 28 (2004) 1142;
[f] J. Fan, H.F. Zhu, T.-a. Okamura, W.Y. Sun, W.X. Tang, N. Ueyama, Chem. Eur. J. 9 (2003) 4724;
[g] G.C. Xu, Y.J. Ding, T.-a. Okamura, Y.Q. Huang, Z.S. Bai, Q. Hua, G.X. Liu, W.Y. Sun, N. Ueyama, Cryst. Growth Des. 9 (2009) 395.
[8] G. Wu, X.F. Wang, T.-a. Okamura, W.Y. Sun, N. Ueyama, Inorg. Chem. 45 (2006) 8523.
[9] [a] J. Fan, W.Y. Sun, T. Okamura, W.X. Tang, N. Ueyama, Inorg. Chem. 42 (2003) 3168;
[b] J. Fan, M.H. Shu, T. Okamura, Y.Z. Li, W.Y. Sun, W.X. Tang, N. Ueyama, New J. Chem. 27 (2003) 1307.
[10] W. Zhao, J. Fan, Y. Song, H. Kawaguchi, T. Okamura, W.Y. Sun, N. Ueyama, Dalton Trans. (2005) 1509.
[11] W. Zhao, J. Fan, T. Okamura, W.Y. Sun, N. Ueyama, Micropor. Mesopor. Mater. 78 (2005) 265.
[12] [a] W.Y. Sun, J. Fan, T. Okamura, J. Xie, K.B. Yu, N. Ueyama, Chem. Eur. J. 7 (2001) 2557;
[b] J. Fan, H.F. Zhu, T. Okamura, W.Y. Sun, W.X. Tang, N. Ueyama, Inorg. Chem. 42 (2003) 158;
[c] J. Fan, B. Sui, T. Okamura, W.Y. Sun, N. Ueyama, J. Chem. Soc., Dalton Trans. (2002) 3868.
[13] S.Y. Wan, J. Fan, T. Okamura, H.F. Zhu, X.M. Ouyang, W.Y. Sun, N. Ueyama, Chem. Commun. (2002) 2520.
[14] A. Altomare, G. Cascarano, G. Giacovazzo, A. Guagliardi, J. Appl. Crystallogr. 26 (1993) 343 SIR92.
[15] DIRDIF94: P.T. Beurskens, G. Admiraal, G. Beurskens, W.P. Bosman, R. de Gelder, R. Israel, J.M.M. Smits, The DIRDIF-program system, Technical Report of the Crystallography Laboratory, University of Nijmegen, The Netherlands, 1994.
[16] teXsan: Crystal Structure Analysis Package, Molecular Structure Corporation, 1999.
[17] J.R. Black, N.R. Champness, W. Levason, G. Reid, Chem. Commun. (1995) 1277.
[18] U.H.F. Bunz, Chem. Rev. 100 (2000) 1605.
[19] M.H.W. Lam, D.Y.K. Lee, S.S.M. Chiu, K.W. Man, W.T. Wong, Eur. J. Inorg. Chem. (2000) 1483.
[20] C.M. Che, C.W. Wan, K.Y. Ho, Z.Y. Zhou, New J. Chem. 25 (2001) 63.
[21] C.M. Che, C.W. Wan, W.Z. Lin, W.Y. Yu, Z.Y. Zhou, W.Y. Lai, S.T. Lee, Chem. Commun. (2001) 721.
[22] F. Neve, A. Crispini, C.D. Pietro, S. Campagna, Organometallics 21 (2002) 3511.
[23] Y.B. Dong, G.X. Jin, M.D. Smith, R.Q. Huang, B Tang, H.C. zur Loye, Inorg. Chem. 41 (2002) 4909.
[24] T. Ren, C. Lin, P. Amalberti, D. Macikenas, J.D. Protasiewicz, J.C. Baum, T.L. Gibson, Inorg. Chem. Commun. 1 (1998) 23.
[25] L.Y. Kong, X.H. Lu, Y.Q. Huang, H. Kawaguchi, Q. Chu, H.F. Zhu, W.Y. Sun, J. Solid State Chem. 180 (2007) 331.
[26] [a] J. Fan, W.Y. Sun, T.-a. Okamura, Y.Q. Zheng, B. Sui, W.X. Tang, N. Ueyama, Cryst. Growth Des. 4 (2004) 579;
[b] G.C. Xu, Y.J. Ding, T.-a. Okamura, Y.Q. Huang, G.X. Liu, W.Y. Sun, N. Ueyama, CrystEngComm 10 (2008) 1052;
[c] G.C. Xu, Q. Hua, T.-a. Okamura, Z.S. Bai, Y.J. Ding, Y.Q. Huang, G.X. Liu, W.Y. Sun, N. Ueyama, CrystEngComm 11 (2009) 261.